Impulse-induced optimum control of escape from a metastable state by periodic secondary excitations

R. Chacón,[1] J. A. Martínez,[2] and J. J. Miralles[3]

[1]*Departamento de Física Aplicada, Escuela de Ingenierías Industriales, Universidad de Extremadura, Apartado Postal 382, E-06006 Badajoz, Spain, EU*

[2]*Departamento de Ingeniería Eléctrica, Electrónica y Automática, Escuela de Ingenieros Industriales, Universidad de Castilla-La Mancha, E-02071 Albacete, Spain, EU*

[3]*Departamento de Física Aplicada, Escuela de Ingenieros Industriales, Universidad de Castilla-La Mancha, E-02071 Albacete, Spain, EU*

(Received 16 February 2012; revised manuscript received 27 April 2012; published 20 June 2012)

We characterize the role of the impulse transmitted (time integral over a half-period) by resonant secondary excitations at controlling (suppressing and enhancing) escape from a potential well, which is induced by periodic primary excitations. By using the universal model of a dissipative Helmholtz oscillator, we demonstrate numerically that optimum control of escape occurs when the impulse transmitted by the chaos-controlling excitations is maximum while keeping their amplitude and period fixed. These findings are in complete agreement with analytical predictions from two independent methods: Melnikov analysis and energy-based analysis. Additional numerical results corresponding to other alternative escape-controlling excitations demonstrate the generality of the essential role of the excitation's impulse.

DOI: 10.1103/PhysRevE.85.066207 PACS number(s): 05.45.Gg, 05.45.Xt

I. INTRODUCTION

Noise-free escape from a potential well is a ubiquitous problem in physics with wide-ranging technological implications where the necessary energy to overcome the energy barrier can be supplied by a periodic excitation. Depending on the excitation's parameters, the escape can, thus, be accomplished by the passage of the system over the barrier which separates the local potential minimum from a neighboring attracting domain. Diverse instances are known in chemistry [1], electrical transport [2], astrophysics [3], and hydrodynamics [4] among many others where escape phenomena can often be well described by a low-dimensional system of differential equations. Indeed, the case that has been most extensively studied in both dissipative and Hamiltonian systems is that in which escape is induced by an escape-inducing (EI) periodic excitation added to the low-dimensional model system so that, before escape, chaotic transients of unpredictable duration (owing to the fractal character of the basin boundary) are usually observed for orbits starting from chaotic generic phase-space regions (such as those surrounding separatrices). In this scenario, the effectiveness of secondary escape-controlling (EC) periodic excitations in suppressing escape has also been demonstrated for the case of the main resonance (between the two excitations involved) in the context of dissipative systems capable of being studied by Melnikov analysis (MA) techniques [5]. This approach was further shown to be useful in the case of incommensurate EC excitations [6]. While early studies in this context have been about the case where both periodic excitations involved are harmonic, the observation that real-world excitations present a great diversity of wave forms suggested studying the effectiveness of EC excitations with different wave forms at suppressing or enhancing escape while keeping their amplitudes and periods constant. Indeed, recent papers provide strong evidence for a different dependence of the EC scenario on harmonic [5] and nonharmonic excitations [7]. In particular, in Ref. [7], it is demonstrated that the EC scenario is highly sensitive to the wave form of periodic secondary excitations. Since there are infinitely many different wave forms, a relevant problem is how to quantitatively characterize the effect of the excitation's wave form on the EC scenario.

In this present paper, we show that a relevant quantity properly characterizing the effectiveness of generic EC periodic excitations $F(t)$ having equidistant zeros in the EC scenario is the impulse transmitted by the excitation over a half-period (hereafter referred to simply as the excitation's impulse [8] $I \equiv \int_0^{T/2} F(t)dt$, T being the period)—a quantity integrating the conjoint effects of the excitation's amplitude, period, and wave form. It is worth mentioning that the relevance of the excitation's impulse has been observed previously in quite different contexts. First, it has been shown that optimum enhancement of ratchet transport [9] (i.e., directed transport by symmetry breaking of zero-mean forces) is achieved when maximal effective (i.e., critical) symmetry breaking occurs, which is, in turn, a consequence of two reshaping-induced competing effects: the increase in the degree of symmetry breaking and the decrease in the (normalized) maximal excitation's impulse, thus, implying the existence of a universal force wave form that optimally enhances ratchet transport [9]. Second, in the context of adiabatically ac driven periodic (Hamiltonian) systems, the width of the separatrix chaotic layer and the adiabatic condition have been shown to depend on the maximal impulse transmitted by the force over a period between two of its consecutive zeros irrespective of its wave form [10]. Third, it has recently been shown, through the examples of driven two-level systems and periodically curved waveguide arrays, that the impulse transmitted by the (effective) force is an essential quantity for the optimum control of the phenomena of coherent destruction of tunneling and dynamic localization [11]. And fourth, the chaotic threshold of a pump-modulation Nd:YVO_4 laser has been shown to be controlled by the modulation impulse [12].

Here, we will discuss the relevance of the impulse transmitted by generic EC excitations by focusing on the case of

the main resonance between the two excitations involved. The rest of this paper is organized as follows. Section II provides the MA-based analytical predictions for the simple model of a dissipative Helmholtz oscillator subjected to a harmonic EI excitation, whereas the EC excitation is given by a periodic function having a variable impulse that is controlled by a single parameter. An energy-based analysis is also included, whose analytical predictions are in complete agreement with those of the MA. Section III provides numerical evidence for the essential role of the excitation's impulse, thus confirming the theoretical approach of Sec. II. The generality of this role of the excitation's impulse is confirmed by the results corresponding to other alternative EC excitations. Our conclusions are presented in Sec. IV.

II. THEORETICAL APPROACH

For the sake of clarity, we concentrate on a simple model for a universal escape situation: a perturbed Helmholtz oscillator [13] described by the equation,

$$\ddot{x} - x + [1 + \eta F(t)]x^2 = -\delta\dot{x} + \gamma\ \sin(\omega t), \tag{1}$$

where all the variables and parameters are dimensionless, and

$$F(t) \equiv N(m)\mathrm{sn}\left[\frac{4Kt}{T} + \Phi\right]\mathrm{dn}\left[\frac{4Kt}{T} + \Phi\right], \tag{2}$$

in which $\mathrm{sn}(\cdot) \equiv \mathrm{sn}(\cdot;m)$ and $\mathrm{dn}(\cdot) \equiv \mathrm{dn}(\cdot;m)$ are Jacobian elliptic functions of parameter m [$K \equiv K(m)$ is the complete elliptic integral of the first kind] [14], $\Phi = \Phi(m,\zeta) \equiv 2K(m)\zeta/\pi$, $\zeta \in [0,2\pi]$, $T \equiv 2\pi/\omega$, and $N(m)$ is a normalization function (see Fig. 1, top) which is introduced for the elliptic excitation to have the same amplitude 1 and period T for any wave form (i.e., $\forall\, m \in [0,1]$). Here, $\gamma\ \sin(\omega t)$ and $\eta x^2 F(t)$ are to be regarded as the EI and EC excitations, respectively. When $m = 0$, then $F(t)_{m=0} = \sin(2\pi t/T + \zeta)$, i.e., one recovers the previously studied case of a harmonic EC excitation [5], whereas, for the limiting value $m = 1$, the excitation vanishes. The effect of renormalization of the elliptic arguments is clear: with T constant, solely the excitation's impulse is varied by increasing the shape parameter m from 0 to 1. Note that, as a function of m, the excitation's impulse,

$$I = I(m,T) \equiv \frac{TN(m)}{2K} \tag{3}$$

presents a single maximum at $m{=}m_{\max}^{\mathrm{impulse}} \simeq 0.717$ (see Fig. 1, bottom). Thus, choice (2) allows one to study the genuine effect on the EC scenario of the impulse transmitted by the EC excitation.

A. Melnikov analysis

We assume that the complete system (1) satisfies the MA requirements, i.e., the dissipation and excitation terms are small-amplitude perturbations of the underlying conservative Helmholtz oscillator $\ddot{x} - x + x^2 = 0$ (see Refs. [15,16] for the general background). It is worth mentioning that the criterion for a homoclinic tangency—accurately predicted by MA in diverse systems [4,17]—is coincident with the change from a smooth to an irregular fractal-looking basin boundary [18]. It is worth noting that these results connect MA predictions

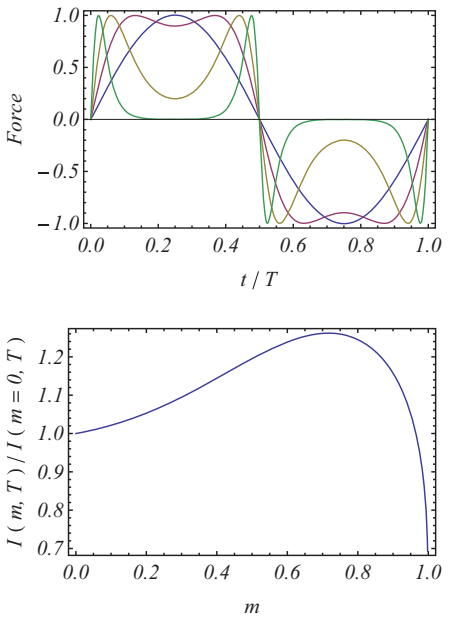

FIG. 1. (Color online) Top: Force $F(t)$ [cf. Eq. (2)] vs t/T, where T is the temporal period and $N(m) \equiv 1/\{a + b/[1 + \exp(\{m - c\}/d)]\}$ with $a \equiv 0.439\,32$, $b \equiv 0.697\,96$, $c \equiv 0.3727$, $d \equiv 0.268\,83$ for $\zeta = 0$ and four values of the shape parameter: $m = 0$ (sinusoidal pulse), $m = 0.72 \simeq m_{\max}^{\mathrm{impulse}} \simeq 0.717$ (nearly square-wave pulse), $m = 0.99$ (double-humped pulse), and $m = 0.999\,999$ (sharp double-humped pulse). Bottom: The normalized excitation's impulse $I(m,T)/I(0,T)$ [cf. Eq. (3)] vs m. The quantities plotted are dimensionless.

with those concerning the erosion of the basin boundary. Straightforward application of MA to Eq. (1) yields the Melnikov function (MF),

$$\begin{aligned} M(t_0) &= -D - A\ \cos(\omega t_0) \\ &\quad + \eta \sum_{n=0}^{\infty} B_n C_n \cos\left[(2n+1)\left(\frac{2\pi t_0}{T} + \zeta\right)\right], \\ D &\equiv \frac{6\delta}{5}, \quad A \equiv 6\pi\gamma\omega^2 \mathrm{csch}(\pi\omega), \\ B_n &\equiv \frac{3}{320}\frac{\pi^3 N(m)\left(n+\frac{1}{2}\right)}{\sqrt{m}K^2(m)}\mathrm{sech}\left[\frac{\left(n+\frac{1}{2}\right)\pi K(1-m)}{K(m)}\right], \\ C_n &\equiv \left[(4n+2)\frac{2\pi}{T}\right]^2\left\{4 + \left[(4n+2)\frac{2\pi}{T}\right]^2\right\} \\ &\quad \times \left\{16 + \left[(4n+2)\frac{2\pi}{T}\right]^2\right\}\mathrm{csch}\left[(2n+1)\frac{2\pi^2}{T}\right]. \end{aligned} \tag{4}$$

Let us assume that, in the absence of any EC excitation ($\eta = 0$), the system (1) undergoes an escape for which the respective MF,

$$M_0(t_0) = -D - A\ \cos(\omega t_0) \tag{5}$$

has simple zeros, i.e., $D \leqslant A$, where the equal sign corresponds to the case of tangency between the stable and the unstable manifolds [16]. If we now let the EC excitation act

on the system such that $B^* \leqslant A - D$, with

$$B^* \equiv \max_{t_0}\left\{\eta\sum_{n=0}^{\infty} B_n C_n \cos\left[(2n+1)\left(\frac{2\pi t_0}{T}+\zeta\right)\right]\right\}, \quad (6)$$

then this relationship represents a sufficient condition for $M(t_0)$ to change sign at some t_0. Thus, a necessary condition for $M(t_0)$ to always have the same sign is

$$B^* > A - D \equiv B_{\min}. \quad (7)$$

Since $B_n > 0$, $C_n > 0$, $n = 0,1,2,\ldots$, one has $B^* \leqslant \eta\sum_{n=0}^{\infty} B_n C_n$ (see the Appendix in Ref. [7]), and hence,

$$\eta > \eta_{\min} \equiv \left(1 - \frac{D}{A}\right)R, \quad R = R(\gamma,T,m) \equiv \frac{A}{\sum_{n=0}^{\infty} B_n C_n}. \quad (8)$$

Equation (10) provides a lower threshold for the amplitude of the EC excitation. Similarly, an upper threshold is obtained by imposing the condition that the EC excitation may not enhance the initial escape, i.e.,

$$B^* \leqslant \eta\sum_{n=0}^{\infty} B_n C_n < A + D \equiv B_{\max}, \quad (9)$$

and hence,

$$\eta < \eta_{\max} \equiv \left(1 + \frac{D}{A}\right)R, \quad (10)$$

which is a necessary condition for $M(t_0)$ to always have the same sign. Thus, the suitable (suppressory) amplitudes of the EC excitation must satisfy

$$\eta_{\min} < \eta < \eta_{\max}. \quad (11)$$

Figure 2 shows how both the threshold amplitudes $\eta_{\min,\max}$ and the width of the range of suitable amplitudes $\Delta\eta \equiv \eta_{\max} - \eta_{\min} = 2(D/A)R$ present a single minimum at $m = m_{\min}$ as the shape parameter m is increased from 0 to 1 due to the dependence of the function R on the shape parameter. While this minimum $m_{\min}$ is very near $m_{\max}^{\text{impulse}} \simeq 0.717$ over a wide range of periods, one cannot expect an exact agreement between $m_{\min}$ and $m_{\max}^{\text{impulse}}$ for all periods owing to the dependence of the chaotic threshold on the common excitation period. This means that ever lower amplitudes $\eta_{\min}$ can suppress escape as the impulse transmitted by the EC excitation approaches its maximum value, whereas the corresponding suppressory ranges $\Delta\eta$ also decrease in the *same* way as $\eta_{\min}$ owing to the impulse-induced enhancement of the escape-inducing effectiveness of the EC excitation.

Regarding suitable values of the initial phase difference ζ, note that ζ determines the relative phase between $M_0(t_0)$ and $\eta\sum_{n=0}^{\infty} B_n C_n \cos[(2n+1)(2\pi t_0/T+\zeta)]$ irrespective of the shape parameter value. We, therefore, conclude from previous theory [19] that a sufficient condition for $\eta_{\min} < \eta < \eta_{\max}$ to also be a sufficient condition for suppressing escape is that $M_0(t_0)$ and $\eta_{\min,\max}\sum_{n=0}^{\infty} B_n C_n \cos[(2n+1)(2\pi t_0/T+\zeta)]$ are in opposition. This yields the optimum suppressory value,

$$\zeta_{\text{opt}}^{\text{sup}} = 0 \quad (12)$$

for all $m \in [0,1]$ in the sense that they allow the widest amplitude ranges for the EC excitation. Similarly, we see that imposing $M_0(t_0)$ to be in phase with $\eta_{\min,\max}\sum_{n=0}^{\infty} B_n C_n \cos[(2n+1)(2\pi t_0/T+\zeta)]$ is a sufficient condition for $M(t_0)$ to change sign at some t_0. This condition provides the optimum enhancer value of the initial phase difference,

$$\zeta_{\text{opt}}^{\text{enh}} = \pi, \quad (13)$$

in the sense that $M(t_0)$ presents its highest maximum at $\zeta_{\text{opt}}^{\text{enh}}$ (i.e., one obtains the maximum gap from the homoclinic tangency condition).

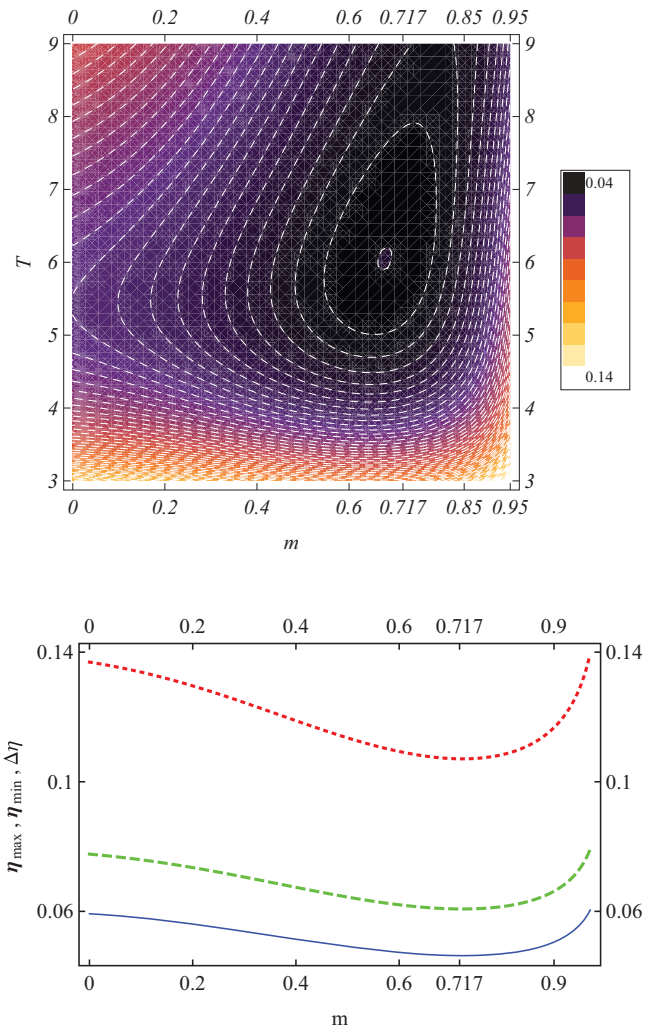

FIG. 2. (Color online) Top: Contour plot of the function $\Delta\eta \equiv \eta_{\max} - \eta_{\min} = 2(D/A)R$ [cf. Eqs. (5) and (8)] vs shape parameter m and period T. Bottom: Eq. (8), solid line: threshold amplitudes $\eta_{\min}$; Eq. (10), dotted line: $\eta_{\max}$; and dashed line: the function $\Delta\eta$ vs shape parameter m for $T = 2\pi/0.85$. System parameters: $\gamma = 0.08$, $\delta = 0.05$. The quantities plotted are dimensionless.

B. Energy-based analysis

By analyzing the variation in the system's energy, one straightforwardly obtains an alternative physical explanation of the foregoing MA-based predictions. Indeed, Eq. (1) has the associated energy equation,

$$\frac{dE}{dt} = -\delta\dot{x}^2 + \gamma\dot{x}\,\sin(\omega t) - \eta\dot{x}x^2F(t), \quad (14)$$

where $E(t) \equiv (1/2)\dot{x}^2(t) + U[x(t)]$ [$U(x) \equiv -x^2/2 + x^3/3$] is the energy function. Integration of Eq. (14) over *any* interval $[nT, nT + T/2]$, $n = 0,1,2,\ldots,$ yields

$$E(nT + T/2) = E(nT) - \delta \int_{nT}^{nT+T/2} \dot{x}^2(t)dt - \eta \int_{nT}^{nT+T/2} \dot{x}(t)x^2(t)F(t)dt + \gamma \int_{nT}^{nT+T/2} \dot{x}(t)\sin(\omega t)dt. \quad (15)$$

Now, if we consider fixing the parameters (δ,γ,T) for the system to undergo an escape at $\eta = 0$, there always exists an $n = n^*$ such that the energy increment $\Delta E \equiv E(n^*T + T/2) - E(n^*T)$ is positive just before escape. Thus, after applying the first mean value theorem [20] together with well-known properties of the Jacobian elliptic functions [14] to the last two integrals on the right-hand side of Eq. (15),

$$E(n^*T + T/2) = E(n^*T) - \delta \int_{n^*T}^{n^*T+T/2} \dot{x}^2(t)dt + \frac{\gamma T}{\pi}\dot{x}(t^*) - \frac{\eta T \dot{x}(t^{**})x^2(t^{**})}{4}F(\zeta,m), \quad (16)$$

where $t^*, t^{**} \in [n^*T, n^*T + T/2]$ and

$$F(\zeta,m) \equiv \frac{N(m)}{K(m)}\mathrm{cn}\left[\frac{2K(m)\zeta}{\pi}\right], \quad (17)$$

with $\mathrm{cn}(\cdot) \equiv \mathrm{cn}(\cdot;m)$ being the Jacobian elliptic function of parameter m, one has

$$\gamma T \dot{x}(t^*)/\pi > \delta \int_{n^*T}^{n^*T+T/2} \dot{x}^2(t)dt,$$

at $\eta = 0$ just before escape. It is straightforward to see that $F(\zeta,m)$ presents an absolute maximum (minimum) at $m = m_{\max}^{\mathrm{impulse}} \simeq 0.717$, $\zeta = 0$ ($m = m_{\max}^{\mathrm{impulse}} \simeq 0.717$, $\zeta = \pi$). It is a 2π-periodic function in ζ and presents the noteworthy properties (see Figs. 3 and 4),

$$\begin{aligned} F(0,m) &= -F(\pi,m) = \frac{N(m)}{K(m)}, \\ F(\pi/2,m) &= F(3\pi/2,m) = 0, \\ \lim_{m\to 1} F(0,m) &= \lim_{m\to 1} F(\pi,m) = 0, \\ \lim_{m\to 0} F(0,m) &= -\lim_{m\to 0} F(\pi,m) = \frac{2}{\pi}. \end{aligned} \quad (18)$$

In this situation, one lets the EC excitation act on the system while holding the remaining parameters constant. For sufficiently small values of $\eta > 0$, one expects that both dissipation work [the integral in Eq. (16)] and $\dot{x}(t^*)$ approximately maintain their initial values (at $\eta = 0$) while the function $F(\zeta,m)$ increases (decreases) from 0 (at $\zeta = \pi/2, 3\pi/2$) so that, in some cases depending upon the remaining parameters (see Figs. 3 and 4), the energy increment just before escape ΔE could be sufficiently large and negative (positive) to suppress (enhance) the initial escape. Clearly, the probability of suppressing (enhancing) the initial escape is maximal at $m = m_{\max}^{\mathrm{impulse}} \simeq 0.717$, $\zeta = 0$ ($\zeta = \pi$) (i.e., when the impulse transmitted by the EC excitation is maximum), which is in complete agreement with the foregoing MA-based predictions.

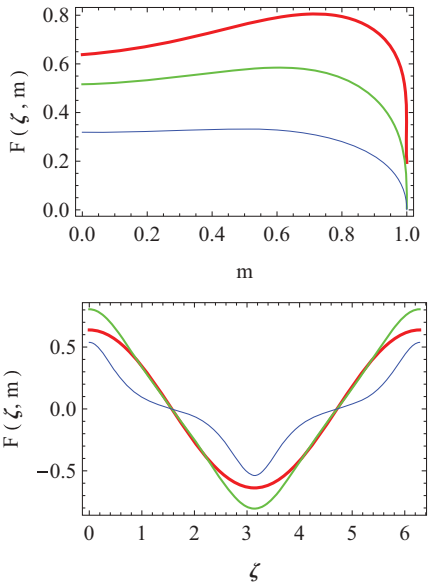

FIG. 3. (Color online) Plots of the function $F(\zeta,m)$ [see Eq. (17)]. Top panel: thick line: F vs m for $\zeta = 0$; medium line: $\zeta = \pi/5$; and thin line: $\zeta = \pi/3$. Bottom panel: thick line: F vs ζ for $m = 0$; medium line: $m = 0.717 \simeq m_{\max}^{\mathrm{impulse}}$; and thin line: $m = 0.99$. The quantities plotted are dimensionless.

III. NUMERICAL RESULTS

For the universal escape model (1), the initial conditions determine, for a fixed set of its parameters, whether the system escapes to an attractor at infinity (with $x \to -\infty$ as $t \to \infty$) or settles into a bounded oscillation. In a series of papers, Thompson and co-workers [4,21,22] have shown for the system,

$$\ddot{x} + x - x^2 = -\delta\dot{x} + \gamma\sin(\omega t), \quad (19)$$

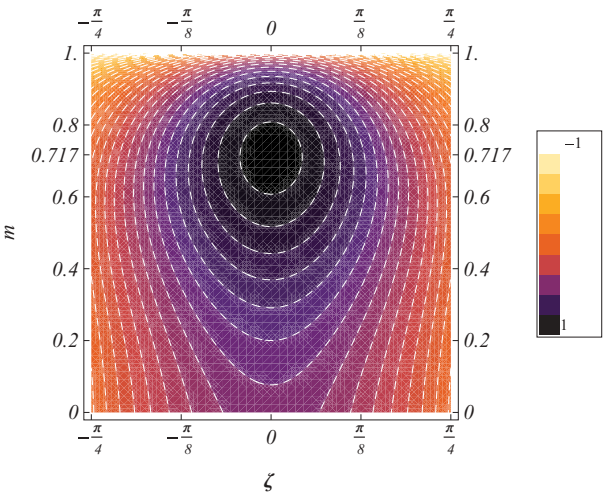

FIG. 4. (Color online) Contour plot of the function $F(\zeta,m)$ [see Eq. (17)] vs ζ and m showing an absolute maximum at $\zeta = 0$, $m = m_{\max}^{\mathrm{impulse}} \simeq 0.717$. The quantities plotted are dimensionless.

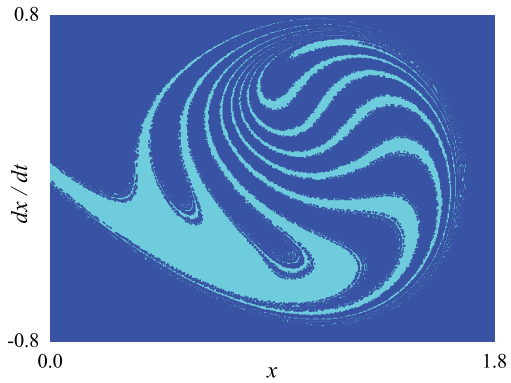

FIG. 5. (Color online) Basin erosion of the system (1) with $\eta = 0$ in the window $0 \leqslant x \leqslant 1.8$, $-0.8 \leqslant \dot{x} \leqslant 0.8$. The color cyan (pale gray) represents the nonescaping basin, and blue (black) represents the escaping basin. System parameters: $\gamma = 0.08$, $\delta = 0.1$, $T = 2\pi/0.85$. The quantities plotted are dimensionless.

that there can exist a dramatic and rapid erosion of the safe basin (union of the basins of the bounded attractors) due to encroachment by the basin of the attractor at infinity (escaping basin). Since the same escape scenario occurs for the closely related system (1) in the absence of an EC excitation ($\eta = 0$), in the following, we show how the degree of erosion of the safe basin can be controlled when $\eta > 0$ according to the MA- and energy-based analysis predictions. The basins of attraction were computed using a fourth-order Runge-Kutta algorithm with time steps in the range of $\Delta t = 0.005 - 0.01$. To numerically generate the basins of attraction, we selected a grid of 400×400 uniformly distributed starting points in the region of phase space $\{x(t=0) \in [0, 1.8],\ \dot{x}(t=0) \in [-0.8, 1]\}$. From this grid of initial conditions, each integration is continued until either $|x|$ exceeds 20, at which point, the system is deemed to have escaped (i.e., to the attractor at infinity) or the maximum allowable number of cycles, here 20, is reached. The color cyan (pale gray) represents the nonescaping basin, and blue (black) represents the escaping basin. In the absence of an EC excitation ($\eta = 0$), the system can be assumed to present a dramatic erosion and stratification of the basin (as in the example shown in Fig. 5).

Figure 6 shows the lowest value of the EC amplitude $\eta'_{\min}$ for which the erosion of the safe basin has completely disappeared as a function of the shape parameter m (dots). One finds a perfect correlation between the inverse of this amplitude $1/\eta'_{\min}$ and the impulse transmitted by the EC excitation [cf. Eq. (3); see Fig. 1, bottom], meaning that the excitation's impulse is the quantity properly controlling the escape from a metastable state. Notably, the experimental points $\eta'_{\min}$ fit the analytical estimate $\eta_{\min}$ [solid line, Eq. (8)]. The increase in $\eta'_{\min}$ is especially fast for values of m very close to 1, which is a consequence of the dependence of $K(m)$ on m [23] [cf. Eq. (2)].

As mentioned in the previous section, the initial phase difference ζ plays a fundamental role in the suppression or enhancement of escape irrespective of the shape parameter value. To test the predictions concerning the dependence of the impulse-controlled escape scenario on ζ, we calculated the escape probability normalized to that of the corresponding

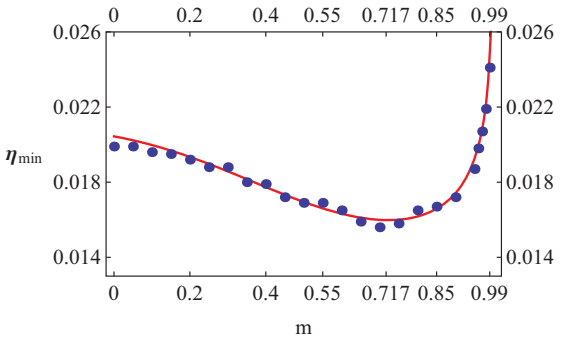

FIG. 6. (Color online) Dots, see the text: lowest value of the EC amplitude η preserving the safe basin without erosion and solid line, Eq. (8): lower threshold for suppression of chaotic escape $\eta_{\min}$ vs shape parameter m. System parameters: $\gamma = 0.08$, $\delta = 0.1$, $T = 2\pi/0.85$. The quantities plotted are dimensionless.

case with no EC excitation $P(\eta > 0)/P(\eta = 0)$ versus ζ for several values of m. Figure 7 shows an illustrative example comparing the cases corresponding to $m = 0$ (harmonic pulse), $m = 0.717 \simeq m_{\max}^{\text{impulse}}$ (nearly square-wave pulse) and $m = 0.999$ (double-humped pulse) in which the numerical results confirm the theoretical predictions of Sec. II. Specifically, one finds, in general, that the wave form associated with the maximum impulse transmitted by the EC excitation has a greater effectiveness at controlling (suppressing and enhancing) escape than any other wave form as predicted. One sees, for the small EC amplitude considered in Fig. 7 $\eta = 0.016$, that such a greater effectiveness is slightly less at the optimum suppressory value of the initial phase difference ($\zeta_{\text{opt}}^{\text{sup}} = 0$) than at the optimum enhancer value ($\zeta_{\text{opt}}^{\text{enh}} = \pi$) (see Fig. 7). Remarkably, the escape scenario is fairly insensitive to the excitation's impulse over certain ranges of the initial phase difference around the values $\zeta = \pi/2, 3\pi/2$, respectively, i.e., those values of the initial phase difference having neither a significant suppressor effect nor a significant enhancer effect [cf. Eq. (18)], confirming, thus, the theoretical predictions of

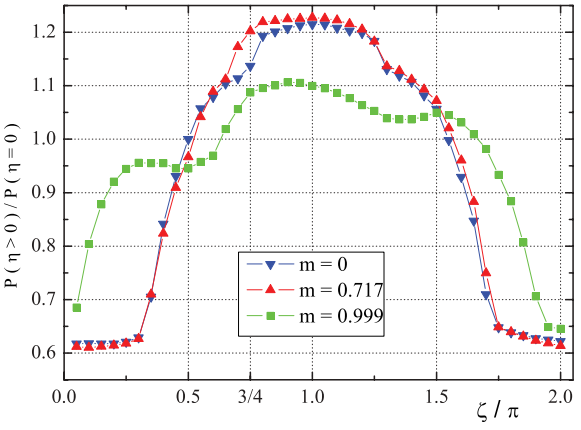

FIG. 7. (Color online) Normalized escape probability (see the text) vs initial phase difference for three values of the shape parameter: $m = 0$ (inverted triangles), $m = 0.717$ (triangles), and $m = 0.999$ (squares). System parameters: $\eta = 0.016$, $\gamma = 0.08$, $\delta = 0.1$, $T = 2\pi/0.85$. Straight lines are solely plotted to guide the eye. The quantities plotted are dimensionless.

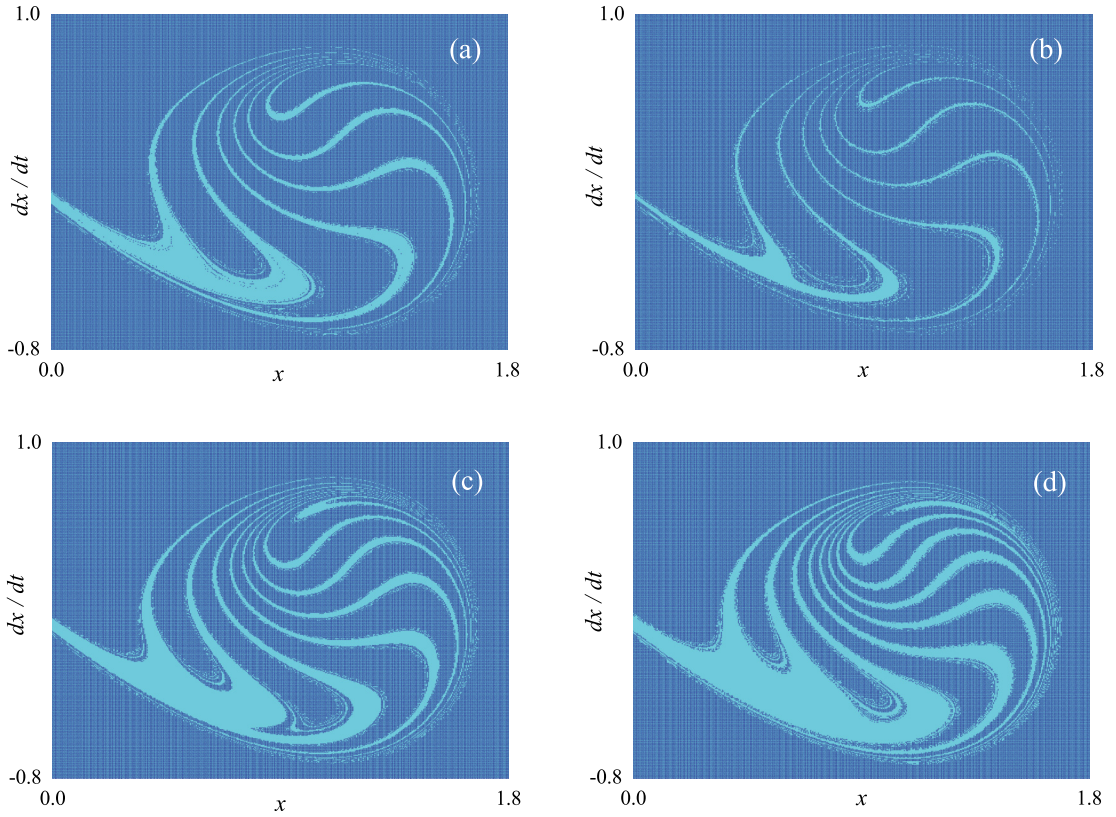

FIG. 8. (Color online) Restoration of the safe basin of the system (1) in the window $0 \leqslant x \leqslant 1.8$, $-0.8 \leqslant \dot{x} \leqslant 1$ for $\eta = 0.016$, $\gamma = 0.08$, $\delta = 0.1$, $T = 2\pi/0.85$, $\zeta = 3\pi/4$, and four values of the shape parameter: (a) $m = 0$, (b) $m = 0.717$, (c) $m = 0.999$, and (d) $m = 1 - 10^{-14}$. The color cyan (pale gray) represents the nonescaping basin, and blue (black) represents the escaping basin.

Sec. II. Our numerical experiments typically show that the excitation's impulse is the quantity properly controlling the erosion and stratification of the safe basin. An illustrative example of impulse-induced enhancement of escape is shown in Fig. 8 for the value $\zeta = 3\pi/4$ (see Fig. 7) and four values of the shape parameter ($m = 0, 0.717, 0.999, 1 - 10^{-14}$). One sees how the safe basin undergoes ever greater erosion as the excitation's impulse approaches its maximum value [$m = 0.717 \simeq m_{\max}^{\text{impulse}}$, Fig. 8(b)] from both harmonic [$m = 0$, Fig. 8(a)] and double-humped [$m = 0.999$, Fig. 8(c); $m = 1 - 10^{-14}$, Fig. 8(d)] pulses.

Next, we provide evidence for the generality of the essential role of the excitation's impulse by considering other alternative EC excitations instead of choices (1) and (2),

$$\ddot{x} - x + x^2 = -\delta\dot{x} + \gamma\,\sin(\omega t) + \eta\gamma F'(t),$$
$$F'(t) \equiv \mathrm{sn}^{2n}\left[\frac{2Kt}{T} + \Xi\right]\mathrm{cn}\left[\frac{2Kt}{T} + \Xi\right], \qquad (20)$$

in which the EC excitation is an external forcing instead of a parametric excitation, $\Xi = \Xi(m,\zeta) \equiv K(m)\zeta/\pi$, $\zeta \in [0,2\pi]$, $T \equiv 2\pi/\omega$, and $n = 1,2,3,\ldots$. For a fixed value of the exponent n, the elliptic excitation $F'(t)$ has the same amplitude (which depends on n) and period T for any wave form (i.e., $\forall\, m \in [0,1]$; see Fig. 9, top). When $m = 0$, then

$$F'(t)_{m=0} = \sin^{2n}(\pi t/T + \zeta/2)\cos(\pi t/T + \zeta/2), \qquad (21)$$

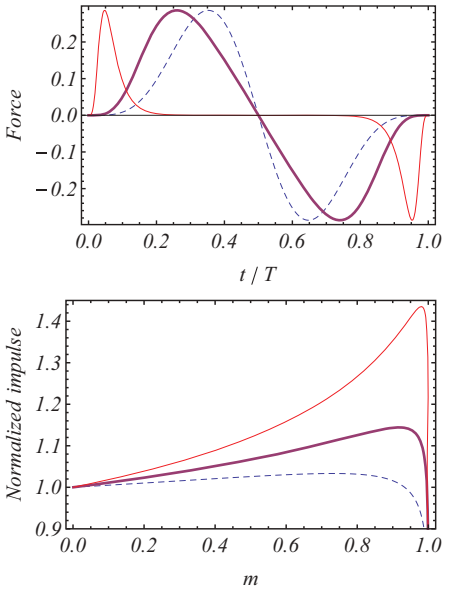

FIG. 9. (Color online) Top: Force $F'(t)$ [cf. Eq. (20)] vs t/T, where T is the temporal period, for $n = 2$, $\zeta = 0$, and three values of the shape parameter: dashed line: $m = 0$, thick line: $m = 0.918 \simeq m_{\max}^{\text{impulse}}(n = 2)$, and sharp pulse: $m = 1 - 10^{-12}$. Bottom: The normalized excitation's impulse $I'(m,T,n)/I'(m = 0,T,n)$ [cf. Eq. (22)] vs m for three values of the exponent: dashed line: $n = 1$, thick line: $n = 2$, and $n = 5$. The quantities plotted are dimensionless.

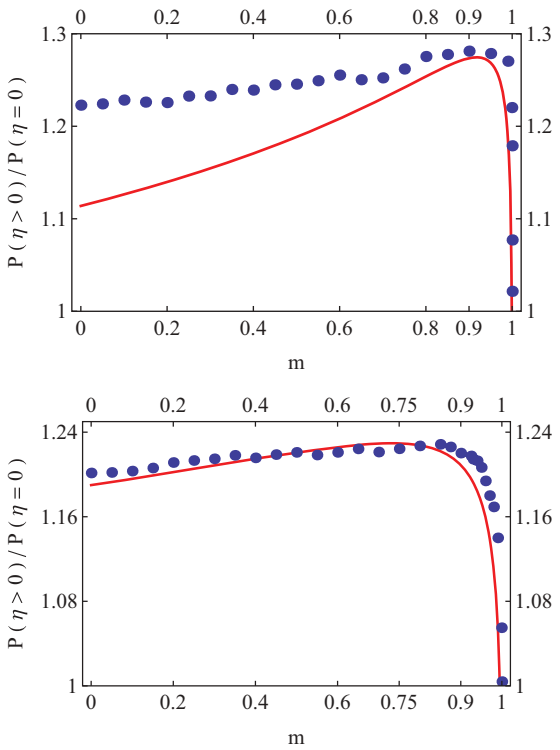

FIG. 10. (Color online) Dots, see the text: Normalized escape probability corresponding to the system (20) and solid lines, cf. Eq. (22): normalized excitation's impulse $cI'(m,T,n)/I'(m=0,T,n)$ vs m for two values of the exponent n. Top: $n=2, c=1.114$, $\eta=0.8$. Bottom: $n=1, c=1.19, \eta=0.4$. System parameters: $\gamma=0.08$, $\delta=0.1$, $T=2\pi/0.85$, $\zeta=0$. The quantities plotted are dimensionless.

whereas, for the limiting value $m=1$, the excitation vanishes. Also, with T and n constant, solely the excitation's impulse is varied by increasing the shape parameter m from 0 to 1. Note that, as a function of m, the excitation's impulse,

$$I' = I'(m,T,n) \equiv T\,\frac{{}_2F_1\left(\frac{1}{2},\frac{2n+1}{2};\frac{2n+3}{2};m\right)}{2(2n+1)K} \qquad (22)$$

presents a single maximum at $m=m_{\max}^{\text{impulse}} \equiv m_{\max}^{\text{impulse}}(n)$ (see Fig. 9, bottom) and where ${}_2F_1(1/2,n+1/2;n+3/2;m)$ is the hypergeometric function [24]. Thus, one has $m_{\max}^{\text{impulse}}(n=1) \simeq 0.730$, $m_{\max}^{\text{impulse}}(n=2) \simeq 0.918$, $m_{\max}^{\text{impulse}}(n=3) \simeq 0.957, \ldots$. In addition to choice (2), the family of functions $\{F'(t)\}_n$ [Eq. (20)] allows one to study the generality of the effect on the EC scenario of the impulse transmitted by the EC excitation. Numerical results corresponding to the Helmholtz oscillator (20) confirm again such an essential role of the excitation's impulse. Figure 10 shows two illustrative examples of a situation where the EC excitation enhances the escape for two values of the exponent n, respectively. In this case, one straightforwardly obtains $\zeta_{\text{opt}}^{\text{enh}}=0\ \forall\, n$, i.e., the optimum enhancer value of the initial phase difference is independent of the exponent n. One finds again that the wave form associated with the maximum impulse transmitted by the EC excitation has a greater effectiveness at enhancing escape than any other wave form as shown in Fig. 10.

IV. CONCLUSIONS

To summarize, we have demonstrated theoretically and numerically that the impulse transmitted by secondary resonant excitations is a fundamental quantity for the optimum control of escape from a metastable state, which is induced by primary periodic excitations. Numerical experiments of a dissipative Helmholtz oscillator showed good agreement with theoretical predictions obtained from two independent approaches: Melnikov analysis and energy-based analysis. Additional numerical experiments corresponding to other alternative escape-controlling excitations demonstrated the generality of the essential role of the excitation's impulse. The present findings can be readily tested experimentally (for instance, in electronic and laser systems [25–27]) and can find application to improve the control of elementary dynamic processes characterized by escape from a metastable state, such as transport phenomena in dissipative lattices or diverse atomic and molecular processes. Future research will be devoted to examining various noisy escape-controlling scenarios in light of the essential role of the excitation's impulse. In particular, this quantity could be useful in the study of Josephson junctions as detectors of periodic signals [28].

ACKNOWLEDGMENTS

The authors gratefully acknowledge partial financial support from the Ministerio de Ciencia e Innovación (MCI, Spain) through Project No. FIS2008-01383 (R.C. and J.A.M.) and from the Junta de Extremadura (JEx, Spain) through Project No. GR10045 (R.C.).

[1] M. E. Goggin and P. W. Milonni, Phys. Rev. A **37**, 796 (1988).
[2] I. Vernik *et al.*, J. Appl. Phys. **81**, 1335 (1997).
[3] G. Contopoulos, H. Handrup, and D. Kaufmann, Physica D **64**, 310 (1993).
[4] J. M. T. Thompson, Proc. R. Soc. London, Ser. A **421**, 195 (1989).
[5] R. Chacón, F. Balibrea, and M. A. López, J. Math. Phys. **37**, 5518 (1996).
[6] R. Chacón and J. A. Martínez, Phys. Rev. E **65**, 036213 (2002).
[7] R. Chacón and J. A. Martínez, Phys. Rev. E **83**, 016201 (2011).
[8] See, e.g., M. Alonso and E. J. Finn, in *Physics* (Addison-Wesley, New York, 1992), p. 118.
[9] R. Chacón, J. Phys. A: Math. Theor. **40**, F413 (2007); **43**, 322001 (2010); P. J. Martínez and R. Chacón, Phys. Rev. Lett. **100**, 144101 (2008); M. Rietmann, R. Carretero-González, and R. Chacón, Phys. Rev. A **83**, 053617 (2011).
[10] R. Chacón, M. Yu. Uleysky, and D. V. Makarov, Europhys. Lett. **90**, 40003 (2010).

[11] R. Chacón, Phys. Rev. A **85**, 013813 (2012).
[12] M.-D. Wei and C.-C. Hsu, Opt. Commun. **285**, 1366 (2012).
[13] H. L. F. Helmholtz, *On the Sensation of Tone as a Physiological Basis for the Theory of Music* (Dover, New York, 1954).
[14] J. V. Armitage and W. F. Eberlein, *Elliptic Functions* (Cambridge University Press, Cambridge, UK, 2006).
[15] V. K. Melnikov, Trans. Moscow Math. Soc. **12**, 1 (1963) [Tr. Mosk. Ova. **12**, 3 (1963)].
[16] J. Guckenheimer and P. J. Holmes, *Nonlinear Oscillations, Dynamical Systems, and Bifurcations of Vector Fields* (Springer, Berlin, 1983).
[17] F. C. Moon and G.-X. Li, Phys. Rev. Lett. **55**, 1439 (1985).
[18] S. W. McDonald, C. Grebogi, E. Ott, and J. A. Yorke, Physica D **17**, 125 (1985).
[19] R. Chacón, *Control of Homoclinic Chaos by Weak Periodic Perturbations* (World Scientific, London, 2005).
[20] I. S. Gradshteyn and I. M. Ryzhik, *Table of Integrals, Series, and Products* (Academic, San Diego, 1980).
[21] J. M. T. Thompson, S. R. Bishop, and L. M. Leung, Phys. Lett. A **121**, 116 (1987).
[22] J. M. T. Thompson and M. S. Soliman, Proc. R. Soc. London, Ser. A **428**, 1 (1990).
[23] M. Abramowitz and I. A. Stegun, *Handbook of Mathematical Functions*, Chap. 17 (Dover, New York, 1972).
[24] M. Abramowitz and I. A. Stegun, *Handbook of Mathematical Functions*, Chap. 15 (Dover, New York, 1972).
[25] R. Meucci, W. Gadomski, M. Ciofini, and F. T. Arecchi, Phys. Rev. E **49**, R2528 (1994).
[26] Z. Qu, G. Hu, G. Yang, and G. Qin, Phys. Rev. Lett. **74**, 1736 (1995).
[27] E. del Río, A. Rodríguez Lozano, and M. G. Velarde, Rev. Sci. Instrum. **63**, 4208 (1992).
[28] P. Addesso, G. Filatrella, and V. Pierro, Phys. Rev. E **85**, 016708 (2012).